Wavefront printing technique with overlapping approach toward high definition holographic image reconstruction

K. Wakunami*[a], R. Oi[a], T. Senoh[a], H. Sasaki[a], Y. Ichihashi[a], K. Yamamoto[a]
[a]National Institute of Information and Communications Technology, 4-2-1, Nukui-Kitamachi, Koganei, Tokyo, 184-8795, Japan

ABSTRACT

A hologram recording technique, generally called as "wavefront printer", has been proposed by several research groups for static three-dimensional (3D) image printing. Because the pixel number of current spatial light modulators (SLMs) is not enough to reconstruct the entire wavefront in recording process, typically, hologram data is divided into a set of sub-hologram data and each wavefront is recorded sequentially as a small sub-hologram cell in tiling manner by using X-Y motorized stage. However since previous works of wavefront printer do not optimize the cell size, the reconstructed images were degraded by obtrusive split line due to visible cell size caused by too large cell size for human eyesight, or by diffraction effect due to discontinuity of phase distribution caused by too small cell size. In this paper, we introduce overlapping recording approach of sub-holograms to achieve both conditions: enough smallness of apparent cell size to make cells invisible and enough largeness of recording cell size to suppress diffraction effect by keeping the phase continuity of reconstructed wavefront. By considering observing condition and optimization of the amount of overlapping and cell size, in the experiment, the proposed approach showed higher quality 3D image reconstruction while the conventional approach suffered visible split lines and cells.

Keywords: Holographic optical element, Electronic holography system, Holographic projection

1. INTRODUCTION

For static 3D visualization, 3D models designed by computer graphics (CG) can be printed out as full-color holograms based on the well-known holographic stereogram (HS) technique [1, 2]. However, HS is based on the recording of dense light-rays and thus, the diffraction effect and spatial/angular sampling of light-rays cause degradation of the reconstructed 3D images, especially target 3D objects/scenes are located far from a hologram plane [3-6]. Therefore, even holography owns potential to full-control of reconstructed wavefront, HS is not a best technique to record an arbitrary wavefront of target 3D models. Recently, a new hologram recording technique, called as wavefront printer, has been proposed by several research groups [7-9]. In wavefront printing technique, since digitally designed wavefront of a target 3D object/scene is optically reproduced by computer generated hologram (CGH) and recorded on the hologram recording material, ideally an arbitrary wavefront with full-control of both amplitude and phase distribution can be recorded. However, because pixel number of current SLM devices is not enough to display the entire hologram data, generally an entire hologram data is divided into a set of sub-hologram data and a wavefront of each is sequentially recorded in tiling manner by using X-Y motorized stage. In this case, phase continuity of recorded/reproduced wavefront is lost between neighboring sub-holograms due to a lack of positioning accuracy of X-Y motorized stage to wavelength of recording light and the time incoherence recording. This phase discontinuity causes the image degradation in reconstruction by diffraction effect at each sub-hologram when the size of sub-holograms is too small. On the other hand, if the size of sub-hologram is too large to the eyesight of observers, the split lines and cells of sub-holograms are visible and this condition also causes the degradation of reconstructed image quality. For the reconstruction of ideal wavefront of target 3D object/scene, the optimization of recording conditions such as the size of sub-holograms, the way to dividing and recording an entire hologram data, should be discussed.

Three-Dimensional Imaging, Visualization, and Display 2016, edited by Bahram Javidi, Jung-Young Son, Proc. of SPIE Vol. 9867, 98670J · © 2016 SPIE · CCC code: 0277-786X/16/$18 · doi: 10.1117/12.2229517

2. PROPOSED APPROACH

2.1 Wavefront printing technique

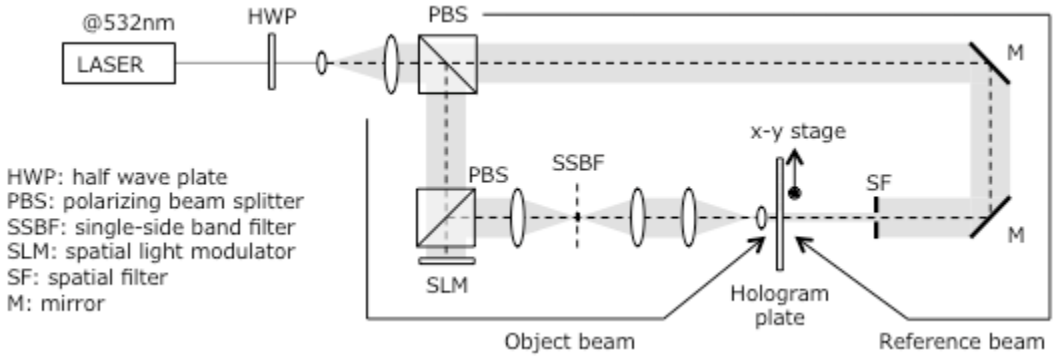

Figure 1. The optical setup of our wavefront printer

At first, the wavefront printing technique is briefly introduced. Fig.1 shows the optical system of our wavefront printer. A collimated light at 532 nm of wavelength is split by polarization beam splitter (PBS) and then, two beams will form an object beam and a reference beam to record a sub-hologram as a reflection-type volume hologram. An object beam is modulated to a wavefront of a part of target 3D objects/scene by sub-hologram data displayed on a spatial light modulator (SLM). Undesirable lights: non-diffraction light and conjugate light, are filtered by single-side band filter and half-zone plate method [10] in the same manner of our electronic holography systems [11, 12]. Then the reduction optical system demagnifies the modulated wavefront on a holographic recording film cobestro Bayfol®HX-102 photopolymer material. A reference beam is formed plane wave and is incident to a holographic recording film from the opposite side of an object beam. Table 1 shows the main parameters of our wavefront printer. Because the pixel number of current SLM is not enough to reproduce an entire wavefront for practical use, the entire hologram data is divided into a set of sub-hologram data and wavefront of each is recorded sequentially in tiling manner by using motorized X-Y stage. After the recording process of all sub-holograms, holographic recording material is then processed by the bleaching so as to own high transmission at visible light wavelength [13].

Table 1. The main parameters of our wavefront printer.

Parameter	Design value
Wavelength of laser	532 [nm]
Pixel number of sub-hologram	3,600 × 1,800 [pixel]
Pixel pitch of SLM	3.5 [μm]
Magnification of reduction optical system	0.10
Hologram recording material	Cobestro, Bayfol®HX-102

2.2 Image degradation due to the phase discontinuity and the visible sub-hologram cells

Within a sub-hologram region, the arbitral wavefront reproduced by CGH can be recorded. However the dividing process of the entire hologram causes the phase discontinuity at the split lines of each sub-hologram due to a lack of positioning accuracy of X-Y motorized stage and also the time incoherence recording of them. Because of this phase discontinuity, the reconstructed image will be degraded by undesired diffraction effect. Here let us consider the required size of phase continuity defined by the size of a sub-hologram to avoid the image degradation under the supposed observing condition. The required size of phase continuity S_P is denoted as the size on the hologram plane in which the reproduced wavefront will be incident to the pupil of the observer's eye (See Fig.2). We suppose that the target object

point is Z_T behind and observing point is Z_O in front of the hologram plane. When the pupil size of the observer's eye is supposed to be D_P, required size of phase continuity area S_P is derived as follow:

$$S_P = \frac{D_P \cdot |Z_T|}{Z_T + Z_O}. \tag{1}$$

If the target point is in front of the hologram, Z_T becomes negative value. Even an entire hologram data is divided into a set of sub-hologram data of the size of S_H, under the following condition, the phase continuity of reconstructed wavefront on the hologram is ensured to the observer, i.e. observers do not recognize the image degradation due to the discontinuity of recorded/reproduced wavefront by the divided hologram. The required condition is

$$\text{Condition 1: } S_P \le S_H . \tag{2}$$

On the other hand, if the size of sub-hologram is larger than the spatial resolution of observer's eyesight, observers will recognize them and the visible cells and split lines will degrade the image quality. Let us consider how size of sub-hologram is resolved by the supposed observing condition with taking visual acuity into account. Here θ_E is denoted as the angular size of the smallest detail observer's eyesight can resolve. On the hologram plane, the size S_E, observers can recognize the detail, is derived as follow:

$$S_E \approx Z_O \cdot \theta_E . \tag{3}$$

To set the size of sub-holograms smaller than the resolution of observer's eyesight, i.e. sub-hologram cells and split lines of them are not visible, the following condition should be satisfied,

$$\text{Condition 2: } S_E \ge S_H . \tag{4}$$

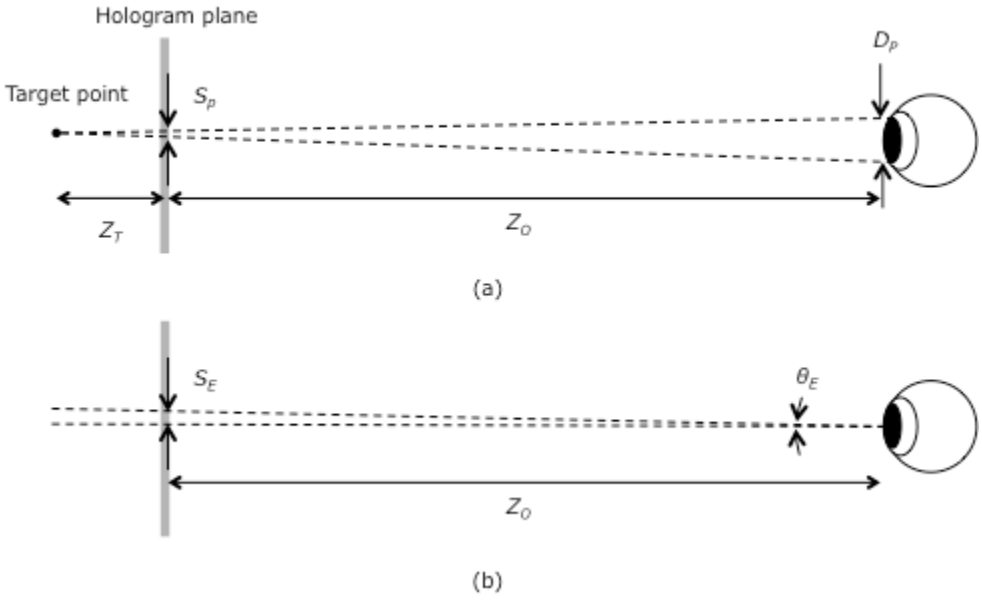

Figure 2. The required cell size of sub-holograms from the viewpoint of two main factors. (a) S_P denotes the required size of phase continuity of wavefront incident to the eye pupil of the observer. (b) S_E denotes the spatial resolution that is defined by using the angular size θ_E of the smallest detail observer's eyesight can resolve.

To satisfy both conditions 1 and 2 to the size of sub-hologram, the image degradation due to the factors discussed above can be suppressed. However, in some practical situations, it is difficult to satisfy both conditions 1 and 2 at the same time. For example, under the following situation that Z_T = 100 mm, Z_O = 1,000mm, D_P = 5.0 mm and θ_P = 1/60 degrees (= 60/60 of the visual acuity), S_P and S_E became almost 0.5 mm and 0.3 mm, respectively. It is clear that the conditions 1 and 2 are conflicting. Therefore any overcoming recording approach to satisfy both conditions is required for high quality 3D image reconstruction.

How about placing the objects in front of the hologram plane?

2.3 Overlapping approach

In this paper, we propose an overlapping approach of recording cells to make it small enough of apparent cell size to observers with still keeping the phase continuity of reconstructed wavefront to the supposed observing condition. Fig.3 shows the concept of proposed approach. Now the entire hologram data is divided into M × N of sub-hologram data considering an overlapping mentioned later. The first exposure of sub-hologram cell (0, 0) is executed on the hologram recording film with the cell size of S_H. In the region of one exposure (gray area in Fig.2), since the recorded wavefront of object light is reproduced from a single SLM, continuity of phase distribution in this region is ensured. Next exposure position of sub-hologram cell (1, 0) is shifted by D_S from sub-hologram cell (0, 0) to X-axis. After recording M times of sub-holograms to X-axis with same shift value D_S, the exposure position of sub-hologram cell (0, 1) is shifted D_S to Y-axis. Then M times of exposure of second line are executed. A repetition of N lines of exposures in the same manner as the first line, the entire hologram can be recorded on the hologram recording film. In the overlapping approach, the phase continuity of wavefront is ensured within the cell size S_H, and the appearance cell size becomes at D_S. Therefore, both parameters can be set independently, and to optimize D_S smaller than S_H, it is possible to keep both conditions 1 and 2. For simple example, if S_H is set at 0.6 mm and D_S is set at 0.3 mm, that is a half of S_H, the conditions 1 and 2 can be satisfied in the example situation described in 2.2.

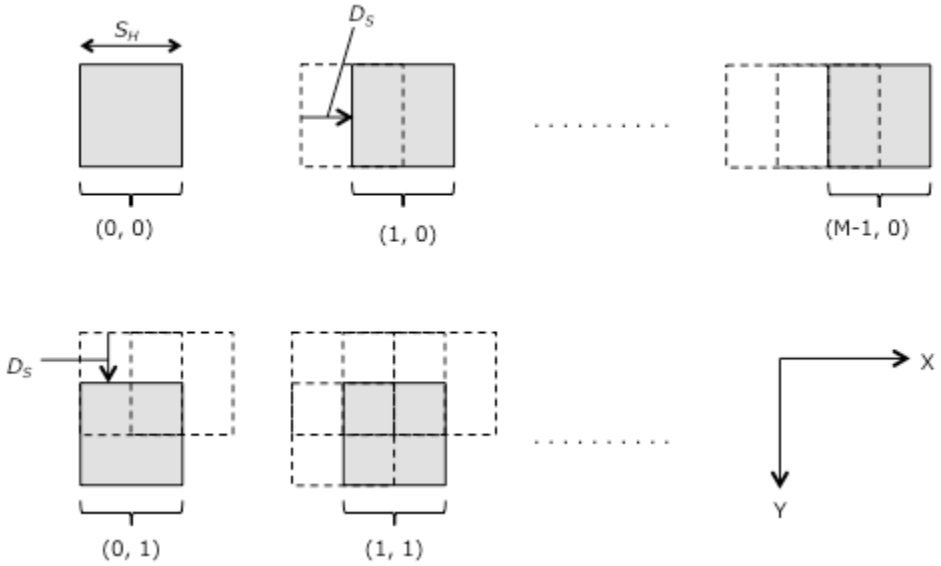

Figure 3. The concept of the overlapping approach. The size S_H within the phase continuity is kept and the apparent cell size D_S can be set at different values independently.

3. EXPERIMENTS

3.1 Verification of overlapping approach

To confirm the effect of overlapping approach, we recorded two holograms by proposed approach and general wavefront printing technique without overlapping of sub-holograms. At first, the entire hologram data was generated based on the holographic stereogram technique [14]. Two 3D objects: the statue of Venus and the characters "NICT" were set behind the hologram and 320 × 320 of perspective images at 256 × 256 pixels were rendered by using the software blender (https://www.blender.org/). The front view image of target 3D scene is depicted in Fig.4 (a). A set of perspective images was then calculated its Fourier spectrum by using fast Fourier transform (FFT) algorithm and the interference patterns of them with reference light were tiled to form the entire hologram data. Total pixel number of hologram data was 81,920 × 81,920 pixels. All of hologram calculation processes from a set of perspective images were executed on the supercomputer TSUBAME2.5 provided by GSIC center in Tokyo Institute of Technology [15].

The entire hologram data was then divided into a set of sub-hologram data for the wavefront printing. Both overlapping approach and non-overlapping approach, sub-hologram data is set at 3,600 × 1,800 pixels. In the proposed approach, half region of overlapping to X and Y axes was employed in the dividing process and thus the total number of sub-holograms was 45 × 91. Because of magnification of reduction optical system of SLM in the wavefront printer, the size of sub-hologram on the hologram recording film became 1.2 × 0.6 mm. Since the overlapping to X and Y axes in the proposed approach, the appearance cell size to the observer became 0.6 × 0.3 mm. Therefore, to Y axis, both conditions 1 and 2 discussed in 2.2 were satisfied theoretically to the example situation described in 2.2. In the conventional recording case, the total number of sub-holograms was 22 × 45 because of non-overlapping, and both recording cell size and the appearance cell size were at 1.2 × 0.6 mm. This means that the phase continuity of wavefront to the observer, the condition 1, could be satisfied but the appearance cell size was too large to the same observing situation in 2.2.

Table 2. Main parameters of the experiment.

Parameter	Design value
Wavelength of laser	532 [nm]
Pixel number of the entire hologram data	81,920 × 81,920 [pixel]
Number of sub-holograms with overlapping / without overlapping	45 × 91 / 22 × 45
Size of the entire hologram	29.4 × 29.4 [mm]

Figure 4. Front view images of original 3DCG data and the optical experimental results.

Fig. 4 (b) and (c) show the results of optical reconstruction of proposed method and the conventional method without overlapping of sub-holograms. It is clear that the case of proposed method (c) reproduced seamless and non-visible cells/split lines of sub-holograms while the conventional case (b) suffered from visible cells that degrades the image quality.

3.2 Large size of wavefront printing at over 77 billion samplings by overlapping approach

For high definition holographic reconstruction, hologram size is also important factor for the practical use. We calculated the hologram data of the wavefront at 10 × 10 cm, and printed out them by wavefront printing technique with overlapping approach. The hologram calculation was executed in the same manner described in 3.1. Because the pixel number of hologram data became as large as 278,528 × 278,528 samples, we divided the entire hologram to 17 × 17 elements and calculated them independently by using multiple CPUs on the supercomputer TSUBAME2.5. Fig. 5 shows the scheme of wavefront printing of 10 × 10 cm hologram. We calculated the hologram data of the real object: the miniature stature of "Buddha" and the virtual CG data "Venus". In the case of "Buddha", 47 of multi-view images were taken from random positions by the camera and then the pictures were combined to generate 3D CG data on the software 123D catch [16].

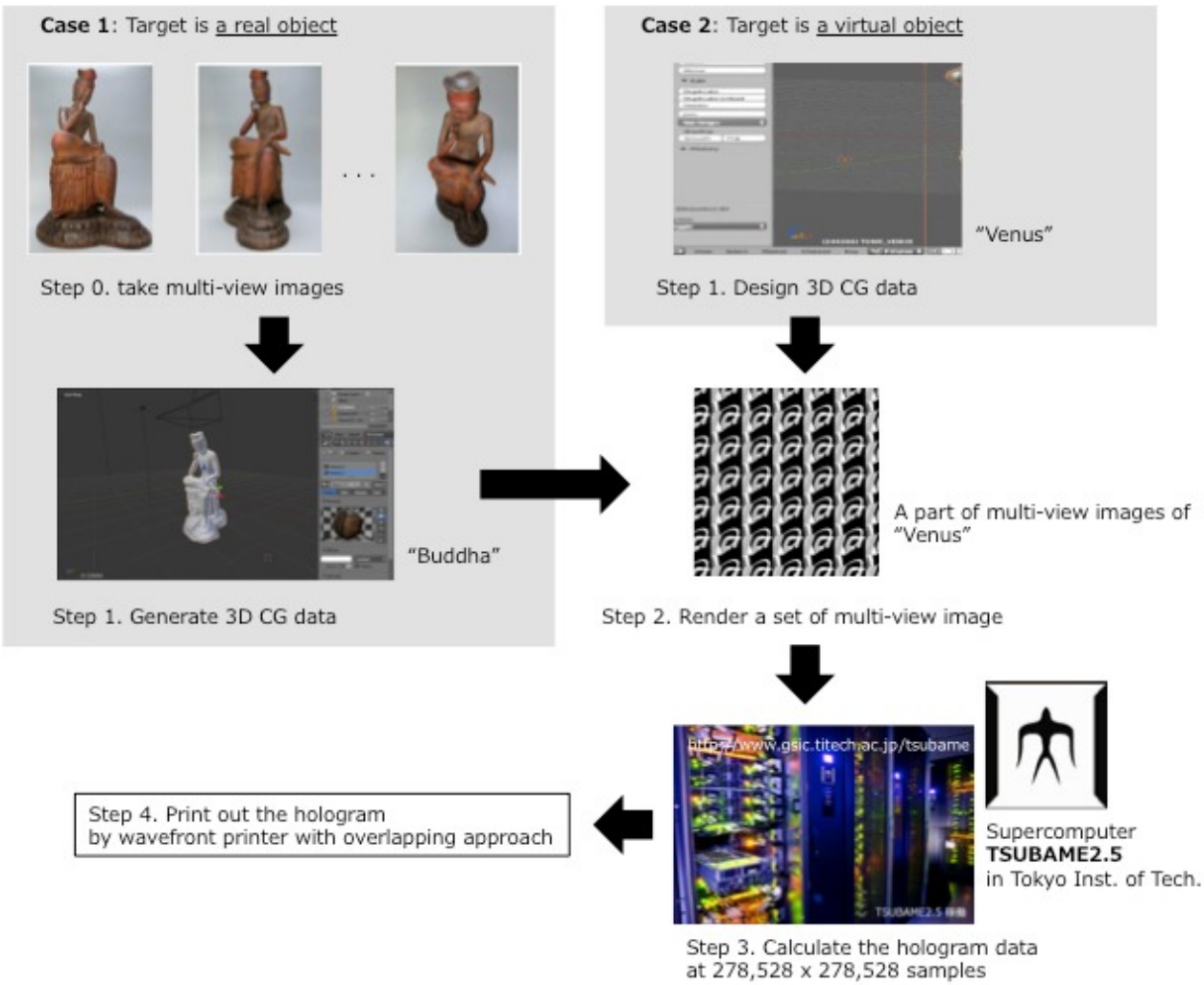

Figure 5. The scheme of wavefront printing at the size of 10 × 10 cm of hologram of a real/virtual object.

Table 3. Main parameters of hologram printing at the size of 10 × 10 cm.

Parameter	Design value
Wavelength of laser	532 [nm]
Pixel number of the entire hologram data	278,528 × 278,528 [pixel]
Number of sub-holograms with overlapping	154 × 309
Size of the entire hologram	100 × 100 [mm]
Number of multi-view images	544 × 544
Pixel number of a view image	512 × 512 [pixel]

Fig.6 shows the results of recorded holograms with overlapping approach. Both real and virtual objects were successfully printed out on the holograms at the size of 10 × 10 cm. Fig.4 (a) shows the comparison between the new hologram of "venus" and the hologram recorded in the previous experiment described in 3.1. Because the recorded

holograms own the wavelength selectivity as a principle of reflection-type volume hologram, the holograms could be reconstructed by using the white illumination light source. The recorded holograms also own high transmission to the visible light after the bleaching process (see Fig.6 (b)).

Figure 6. The results of optical reconstruction. (a) Comparison between the holograms at the size of 10.0 × 10.0 cm and 2.9 × 2.9 cm. (b) and (c) The optically reconstructed image of "Venus" and "Buddha".

4. DISCUSSIONS AND FUTURE WORK

In the overlapping approach, sub-holograms were multiply recorded on the hologram recording film. This multiple exposures caused the decreasing of the diffraction efficiency (D. E.) due to the finite dynamic range of the recording material. To avoid undesirable decreasing of D.E., we will handle to establish the optimization of overlapping parameters that takes the number of overlapping into account. Full-color wavefront printing will be also focused on in our future work.

ACKNOWLEDGMENT

This work was supported by JSPS KAKENHI Grant Number 26790064. This work was supported by JSPS KAKENHI Grant Number 16H01742. This research is supported by the Center of Innovation Program from Japan Science and Technology Agency, JST. The numerical calculations were carried out on the TSUBAME2.5 supercomputer in the Tokyo Institute of Technology.

REFERENCES

[1] Zebra imaging, "We Make 3D Holographic Prints from 3D Models." http://www.zebraimaging.com/ (2016).
[2] Holoxica, "Digital 3D Holograms." http://www.holoxica.com/ (2016).
[3] McCrickerd, J. T., "Comparison of Stereograms: Pinhole, Fly's Eye, and Holographic Types," J. Opt. Soc. Am. A **62**, 1, 64-70 (1972).
[4] Helseh, L. E., "Optical transfer function of three-dimensional display systems," J. Opt. Am. A **23**, 4, 816-820 (2006).
[5] Hilaire, P. St., "Modulation transfer function and optimum sampling of holographic stereograms," Appl. Opt. **33**, 5, 768-774 (1994).
[6] Wakunami, K. and Yamaguchi, M., "Calculation for computer generated hologram using ray-sampling plane," Opt. Exp. **19**, 9086 (2011).
[7] Yamaguchi, T. Miyamoto, O. & Yoshikawa, H. "Volume hologram printer to record the wavefront of three-dimensional objects" Opt. Eng. **51**, 7 (2012).

[8] Nishi, W & Matsuashima, K. "A wavefront printer using phase-only spatial light modulator for producing computer-generated volume holograms" Proc. SPIE **9006**, 90061F (2014).
[9] Kim, Y. et al. "Seamless full color holographic printing method based on spatial partitioning of SLM" Optics Express, **23**, 1 (2015).
[10] Bryngdahl, O. & Lohmann, "A. Single-Sideband Holography" J. Opt. Soc. Am. **58**, 620-624 (1968).
[11] Senoh, T. et al. "Wide viewing-zone angle full-color electronic holography system using very high resolution liquid crystal display panels" Proc. SPIE **7957,** 795709 (2011).
[12] Sasaki, H. et al. "Large size three-dimensional video by electronic holography using multiple spatial light modulators" Scientific Reports, **4**, 6177 (2014).
[13] Berneth, H. et al. "Bayfol HX photopolymer for full-color transmission volume Bragg gratings" Proc. SPIE **9006**, 900602 (2014).
[14] Yatagai, T. "Stereoscopic approach to 3-D display using computer-generated hologram" Applied Optics **15**, 11 (1976).
[15] Tokyo Institute of Technology, Global Scientific Information and Computing Center, "TSUBAME2.5." http://www.gsic.titech.ac.jp/en (2016).
[16] AUTODESK, "123D Catch is a free app that lets you create 3D scans of virtually any object." http://www.123dapp.com/catch (2016).